PERINTIS eJournal

PERINTIS eJournal, **2020**, Vol. 10, No. 1, pp. 50-68

EFFECT OF HALLOYSITE NANOTUBES ON THE MECHANICAL, PHYSICAL AND THERMAL PROPERTIES OF IMPACT MODIFIED POLY(LACTIC ACID)

Ang Hock Tee[1], Zainoha Zakaria[1*], Muhammad Akmal Ahmad Saidi[2], Azman Hassan[2]

[1]Department of Chemistry, Faculty of Science, Universiti Teknologi Malaysia, 81310 Johor Bahru, Malaysia
[2]School of Chemical and Energy Engineering, Faculty of Engineering, Universiti Teknologi Malaysia, 81310 Johor Bahru, Malaysia

* Corresponding author: zainoha@kimia.fs.utm.my

ABSTRACT

Halloysite nanotubes (HNT) has gained much attention for research due to its reinforcing effect in mechanical properties, thermal stability, and nucleating effect. In this study, poly(lactic acid)/core-shell rubber/halloysite nanotubes (PLA/CSR/HNT) nanocomposites were prepared through melt blending, followed by compression molding and cut into different test specimens according to ASTM standards. The incorporation of HNT was performed at different content (0.5, 1.0, 1.5 and 2.0 phr) to study the effect of HNT content on mechanical, physical and thermal properties of impact modified PLA (PLA/CSR). It was found that the flexural strength of impact modified PLA improved significantly by 26.3% when 1.0 phr of HNT was incorporated while the flexural modulus recorded the highest reading at 1955 MPa by the incorporation of 0.5 phr HNT. The results revealed that agglomeration caused by higher content of HNT decreased the flexural properties of PLA/CSR/HNT compared to PLA/CSR. The water absorption and biodegradability of PLA/CSR/HNT were improved, primarily due to the hydrophilic nature of HNT which promoted the interaction with water molecules. From TGA results, 2.0 phr HNT was reported to greatly improve the thermal stability of PLA/CSR/HNT by a higher shift of degradation temperature. Based on DSC thermograms, a decline in the degree of crystallinity of PLA/CSR/HNT was observed when HNT was incorporated which could be due to inhibition of crystallization by HNT in PLA/CSR/HNT nanocomposites. In conclusion, incorporation of HNT at low content into impact modified PLA showed appreciable improvement in the mechanical, physical, and thermal properties of impact modified PLA.

Keywords: *Halloysite nanotubes; poly(lactic acid); flexural properties; water absorption; thermal properties*

1.0 INTRODUCTION

Since the usage of plastics is not totally avoidable in modern life, bio-based and biodegradable polymers from renewable resources for example polyglycolic acid, polyvinyl alcohol, and poly(lactic acid) (PLA) have received an increasing amount of attention as a replacement for conventional petroleum-based plastics, predominantly due to environmental concerns and realization that our petroleum resources are finite [1, 2]. Among these, PLA is one of the most promising polymers due to its sought-after properties such as biodegradability and ability to be derived from renewable resources, in particular agriculture products [1]. The other reasons why PLA gained its popularity among the researchers are because of its notable performances such as high stiffness and strength, good transparency and compostability [3]. PLA has been proved to be water resistant which makes it reasonably suitable for food packaging and it is classified under Generally Recognized as Safe category. For these reasons, PLA has commercially become a replacement for poly(ethylene terephthalate) and polystyrene in many traditional application areas such as fibers, foamed food trays, thermoformed packaging, thermoplastics and housing for computers and electronics [4].

In spite of that, there are also a few major drawbacks associated with PLA. PLA is found to have low impact strength, low heat resistance, and low crystallization rate as compared to conventional thermoplastic. These limitations have restricted the usage of PLA in a wider range of application [3]. To address these limitations, some approaches have been performed to enhance the thermal and mechanical properties of PLA, which including the incorporation of fillers (micro- or nano-), bio-based materials (natural fibers) and other polymers (such as impact modifiers) into PLA [1]. The low impact strength of PLA can be overcome by adding impact modifier to PLA [5]. On the other hand, the reinforcement of PLA using mineral fillers is a common technique in order to reduce the cost of production besides imparting improvements in thermal and mechanical properties of PLA. Many studies have been reported on the application of mineral fillers, such as talc [6], basalt [7], calcium carbonate [8], dolomite [9,10], nanoclay [11], and HNT [5], as fillers in PLA.

Halloysite nanotube (HNT) is an abundantly available natural nanomaterial with rod-like structure that consist of nanoscale lumens and high length-to-diameter (L/D) ratio which makes it attractive for technological applications and polymer reinforcement [12]. HNT has been reported to successfully enhanced the mechanical, thermal, crystallization, and other specific properties for various polymers such as polypropylene (PP) [13], polyamide (PA) [12,14], polybutylene terephthalate (PBT) [12,15] and linear low density polyethylene (LLDPE) [16] by acting as a reinforcing filler and nucleating agent [17]. It is also found that HNT provides an effective interfacial interaction with polar polymers due to the hydroxyl and siloxane functional groups that form hydrogen bonding with the matrix [12,18].

Many researchers had investigated the effect of HNT on the mechanical, physical, thermal, and structural properties of PLA. However, no study was reported on the combination of HNT as filler and core-shell rubber (CSR) as impact modifier for PLA. Therefore, it is of interest to investigate the effect of HNT and CSR on mechanical, physical, thermal, and structural properties of PLA. Moreover, the naturally available HNT and CSR are expected to be beneficial to the food packaging industry due to its non-toxicity and eco-friendly properties when combined with PLA.

2.0 METHODOLOGY

2.1 Materials

PLA (Ingeo Biopolymer 3001D) in pellet form with a density of 1.24 g/cm^3 and melt flow rate (MFR) of 22 g/10 min (at 210 °C, 2.16 kg) was obtained from Nature Work^{TM}, Minnetonka (USA). The additives used for polymer blending in this study were CSR and HNT. The impact modifier, CSR (Paraloid EXL^{TM} 2330) was purchased from Dow Inc. (USA) in white powdered solid form with a density of 1.11 g/cm^3 and melting point of 132-149 °C. HNT (also known as kaolin clay) with a diameter of 30-70 nm, length of 1-3 µm, and pore size of 1.26-1.34 mL/g pore volume was purchased from Sigma-Aldrich (M) Sdn. Bhd. to be used as nanofiller.

2.2 Preparation of PLA/CSR/HNT Composites

All the raw materials (PLA, HNT, and CSR) were weighed according to the formulations presented in Table 1 and dried in an oven at 40 °C for 24 hours to remove the moisture prior to the melt blending process. The raw materials were then premixed, followed by the melt extrusion using a co-rotating twin screw extruder (Werner & Pfleiderer ZSK25, Germany). The temperature settings for compounding all of the nanocomposites were 160/175/190/200 °C from the feed section to die with a rotating screw speed of 50 rpm. The extruded strand was then air-dried and pelletized. Later, the pelletized PLA nanocomposites were compression molded at 190 °C by using a laboratory motor hydraulic hot press (Guthrie, Malaysia) into a 180 mm × 180 mm square plate of 1 mm and 3 mm thickness. The preheating, compressing and cooling time were fixed at 2 minutes, 3 minutes and 5 minutes respectively. The square plates were then cut into different dimension for sample analysis using a band saw.

Table 1 Formulation of PLA/CSR/HNT nanocomposites.

Material Designation	PLA (wt%)	CSR (wt%)	HNT (phr)
PLA	100	0	0
PLAC	95	5	0
PLACH0.5	95	5	0.5
PLACH1.0	95	5	1.0
PLACH1.5	95	5	1.5
PLACH2.0	95	5	2.0

2.3 Sample Analysis

2.3.1 Mechanical Properties

Rectangular-shaped bars of 127.0 mm × 12.7 mm × 3.0 mm (length × width × thickness) were cut from the compression molded PLA/CSR/HNT plates for flexural test in accordance with ASTM D790 standard method. The test specimens were conditioned at 23 ± 2 ℃ and 50 ± 5% humidity for more than 40 hours prior to test. The dimensions of the specimens were carefully measured using a digital caliper and recorded. The span length was set at a span-to-depth ratio of 16 as required by the standard. Next, the test was carried out in ambient temperature using a universal testing machine (Zwick/Roell Z02) at test speed of 2 mm/min with a 20kN load cell. At least 5 specimens for each formulation were tested and reported. From the test report, the flexural strength and flexural modulus were determined.

2.3.2 Physical Properties

2.3.2.1 Water Absorption Test

The test specimens 20.0 × 20.0 × 3.0 mm (length × width × thickness) were cut from the compression molded square plate and oven dried at 50 ℃ until a constant weight was obtained, and immediately weighed to the nearest 0.001 g. The conditioned specimens were then immersed in a container filled with water and placed in a thermostated stainless steel water bath, maintained at two different temperatures, which are 30 ℃ and 50 ℃, for two weeks. The changes on weight were recorded on daily basis by removal of the specimens from the water bath. When all the specimens were removed from the water, the water on the surface was wiped off with a dry cloth, and immediately weighed to the nearest 0.001 g. The percentage change of weight (M_t) at any time, as a result of water absorption was determined using Equation 1.

$$M_t = \left({}^{w_w - w_d}/_{w_d}\right) \times 100\% \quad (1)$$

where w_w is the weight of wet samples (after immersion in water); and w_d is initial weight of dry samples (before immersion).

2.3.2.2 Soil Burial Test

Soil burial test was carried out based on the method published by Thakore, Desai [19] with slight modification to evaluate the biodegradability of the PLA nanocomposites in natural environment condition. Test specimens of 20.0 × 20.0 × 2.0 mm (length × width × thickness) were prepared from the compression molded materials. The samples were then dried in an oven at 50 ℃ until a constant weight (w_i) was attained. The samples were then buried under the soil at a depth of approximately 10.0 cm for a duration of 17 weeks. The soil was sprayed with water daily to maintain the moisture content. Weight measurement was performed by an analytical balance after soil burial test. Upon removal, the samples were washed with distilled water to remove the adherent soil. The samples were dried in a vacuum oven at 50 ℃ and kept in desiccator until a constant weight (w_t) was obtained. The percentage of weight lost (WL) was determined using the Equation 2.

$$\mathrm{WL} = \left({}^{w_i - w_t}/_{w_i}\right) \times 100\% \qquad (2)$$

where w_i is initial dry weight before degradation; and w_t is residual dry weight after degradation at exposure time t.

2.3.3 Thermal Properties

2.3.3.1 Thermogravimetric Analysis

Thermogravimetric analysis (TGA) was used to investigate the thermal stability of the composite. The amount of mass loss of the PLA/CSR/HNT composite when subjected to heating was determined in TGA test using TGA/DSC3$^+$ Mettler Toledo Star^e system with alumina crucible using approximately 10 to 15 mg of sample. The analysis was conducted within temperature range of 30 ℃ to 600 ℃ at a heating rate of 10 ℃/min under nitrogen atmosphere.

2.3.3.2 Differential Scanning Calorimetry

Differential scanning calorimetry (DSC) was carried out using TA DSC 25 (TA instruments, USA). The samples (≈5 mg) were heated from 25 to 250 ℃ at a rate of 10 ℃/min. The DSC cell was constantly purged with nitrogen at a flow rate of 50 mL/min. By referring to DSC thermograms, the glass transition temperature (T_g), crystallization temperature (T_c), melting temperature (T_m), enthalpy of cold crystallization (ΔH_{cc}) and the enthalpy of melting (ΔH_m) were determined with the aid of TA instruments TRIOS software. The relative degree of crystallinity (χ_c) was then calculated using the Equation 3.

$$X_c = \left({\Delta H_m - \Delta H_{cc}} \Big/ {\Delta H_f \times w_{PLA}} \right) \times 100\% \quad (3)$$

where ΔH_m is enthalpy of melting, ΔH_{cc} is enthalpy of cold crystallization, ΔH_f is enthalpy of fusion for 100% crystalline PLA; and w_{PLA} is the weight fraction of PLA in the nanocomposites. The enthalpy of fusion for 100% crystalline PLA material is approximately 93.6 J/g as reported previously [20].

2.3.4 Attenuated Total Reflectance-Fourier Transform Infrared Spectroscopy

Attenuated Total Reflectance-Fourier Transform Infrared Spectroscopy (ATR-FTIR) was performed to characterize the chemical compositions of PLA/CSR/HNT nanocomposites with different HNT content. The samples were scanned within wavenumber range of 650 to 4000 cm^{-1} using a Perkin Elmer FTIR Spectrometer Frontier. All spectra were obtained with a resolution of 8 cm^{-1} and 8 scans.

3.0 RESULTS AND DISCUSSION

3.1 Flexural Properties

In general, the flexural strength represents the maximum stress experienced within the material before it yields in a flexural test, whereas the flexural modulus indicates the stiffness of a material, revealing its tendency to resist bending. Based on flexural test result, a neat PLA has a flexural strength of 17.7 MPa and a flexural modulus of 1965 MPa. This observation is inconsistent with the observation reported by Akbari et. al. [12], which recorded a flexural strength of 95 MPa and a flexural modulus of 3500 MPa. The flexural strength and modulus of neat PLA in this study are apparently lower than the result reported in their study, probably due to the different processing techniques. In this study, compression molding technique was utilized compared to the study by Akbari et. al. [21] which utilized injection molding. According to Aversa et. al. [22], during compression molding, there are probability of nonoptimal melting of pellets which could lead to the presence of boundary layers and voids between the grains. As a result, low flexural properties obtained due to the ineffective stress transfer.

The effects of CSR on flexural strength and flexural modulus of PLA are shown in Figure 1. The addition of 5 wt% CSR into PLA diminished the flexural strength and flexural modulus of neat PLA by 11.9% and 4.5% respectively. This is expected due to the rubbery nature of the CSR which exhibits lower flexural properties than neat PLA. Similar results were reported by Taib et. al. [23]. Another reason for the decreased in flexural properties of PLA/CSR composite is most probably to the lowering of crystallinity by CSR as seen in DSC results.

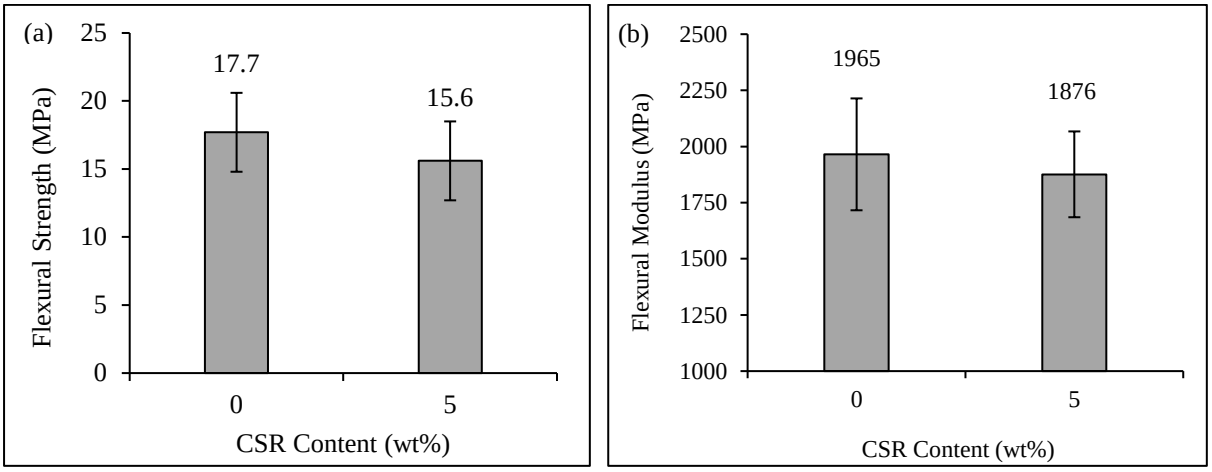

Figure 1 Effect of CSR content on (a) flexural strength and (b) flexural modulus of PLA.

The reinforcing effect of HNT on polymer, frequently observed at low content, is often associated with its rod-like and high aspect ratio structure. Nevertheless, the interfacial properties (nanotube-polyester matrix) can contribute to the improvement of physical properties [24]. Figure 2 demonstrate the effects of HNT on flexural strength and flexural modulus of PLA/CSR at different contents. It can be seen that the flexural strength of PLA/CSR increased with the increasing HNT contents up to 1.0 phr HNT (19.7 MPa). This increase in flexural strength can be attributed to the interaction between PLA and HNT, which facilitating the transfer of stress generated in PLA matrix to HNT which act as the reinforcing phase. However, the further increase in HNT content had caused a slight decrease on the flexural strength. In any case, these values are still higher than that of PLA/CSR. Thereafter, the possible reason for the decrease in flexural strength with increasing HNT content could be due to the increase in agglomeration of HNT when concentration increases. This leads to poor dispersion of HNT in PLA matrix and become stress concentration points for deteriorating mechanical properties [25].

On the other hand, the incorporation of HNT had also improved the flexural modulus of PLA/CSR as shown in Figure 2. It is noteworthy mentioning that the incorporation of HNT at 0.5 and 1.0 phr have successfully increased the flexural modulus of PLA/CSR by 4.2% and 0.2% respectively. The highest flexural modulus was recorded at 1955 MPa when 0.5 phr of HNT was incorporated into PLA/CSR. This phenomenon can be attributed to the reinforcing effect and rigidity of HNT [17]. Similar to flexural strength, the further increase in HNT content (1.0, 1.5 and 2.0 phr) had caused a decrease on the flexural modulus, while 1.5 and 2.0 phr HNT showed a flexural modulus of 1794 MPa and 1793 MPa respectively, which were lower than those of PLA/CSR.

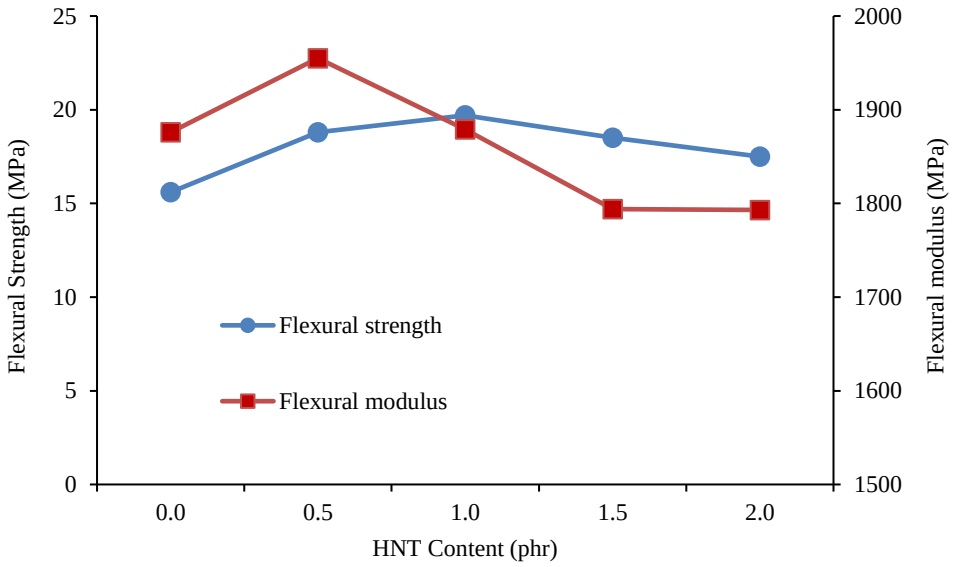

Figure 2 Effect of HNT on flexural strength and flexural modulus of PLA/CSR at different content.

3.2 Water Absorption

Table 2 summarizes the water absorption of PLA and its nanocomposites at immersion temperature of 30 ℃ and 50 ℃. The water absorption test was carried out for 2 weeks and the daily water absorption of PLA/CSR/HNT nanocomposites at immersion temperature of 30 ℃ and 50 ℃ are shown in Figure 3 and 4, respectively. A rapid water absorption was observed for all the specimens, especially during the first few days of immersion and subsequently followed by saturation along the test. It is commonly believed that the hydrophilicity of PLA ester groups will increase the water absorption. At immersion temperature of 30 ℃, neat PLA recorded a total of 1.03 % of water absorption after 2 weeks. It can be seen that the addition of CSR decreased the total water absorption of neat PLA by 0.18 % possibly due to the physical hindrance of CSR to the diffusion of water molecules. However, the incorporation of HNT had permitted an overall increase in maximum water absorption in PLA/CSR. Among all PLA/CSR/HNT composites, HNT content at 0.5 phr showed the highest percentage of maximum water absorption at 0.97%. This indicates that HNT is prone to water absorption, which can be directly attributed to its hydrophilic nature (existence of Al-OH and Si-O-Si groups) which are available for interactions with water molecules [26].

Water absorption test at immersion temperature of 50 ℃ is often referred as hygrothermal aging test. Hygrothermal aging is a degradation process which combines the effect of moisture and temperature, resulting in substantial weight loss and deterioration of mechanical properties [27]. According to Ishak and Berry [28], the exposure of the composite to a hot and moist

environment will only activate the moisture penetration (i.e, diffusion) mechanism after the occurrence of specific damage to the composites. In overall, the water absorption of PLA and its nanocomposites were significantly higher at the immersion temperature of 50 ℃. The addition of CSR had reduced the water absorption of PLA at 50 ℃. When HNT was incorporated into PLA/CSR, the water absorption was increased with the increasing HNT content. The highest water absorption was recorded at 3.01% by PLA/CSR with 2.0 phr HNT. The swellability and absorption ability of HNT which are temperature dependent could be addressed as an important factor contributing to the increasing water absorption at 50 ℃ [26]. In other words, higher temperature increases the swelling of HNT structure, creating numbers of microvoids in PLA matrix and subsequently induces higher water absorption.

Table 2 Water absorption of PLA and its nanocomposites.

Material Designation	**Total Water Absorption After 2 Weeks, M_t (%)**	
	30 ℃	**50 ℃**
PLA	1.03 ± 0.04	2.19 ± 0.06
PLAC	0.85 ± 0.02	2.13 ± 0.08
PLACH0.5	0.97 ± 0.04	2.13 ± 0.08
PLACH1.0	0.91 ± 0.00	2.15 ± 0.08
PLACH1.5	0.92 ± 0.09	2.16 ± 0.16
PLACH2.0	0.93 ± 0.02	3.01 ± 0.06

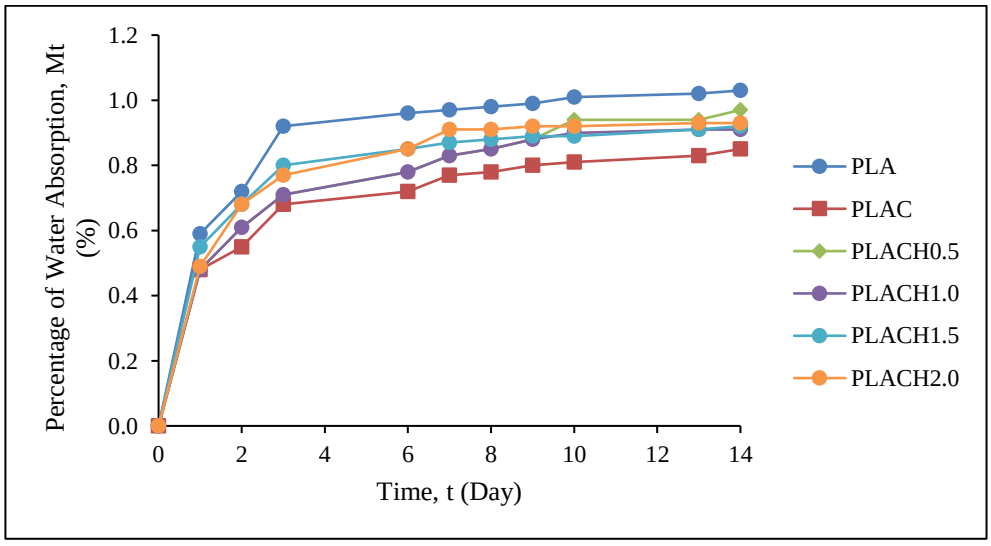

Figure 3 Water absorption of PLA and its nanocomposites at immersion temperature of 30 ℃

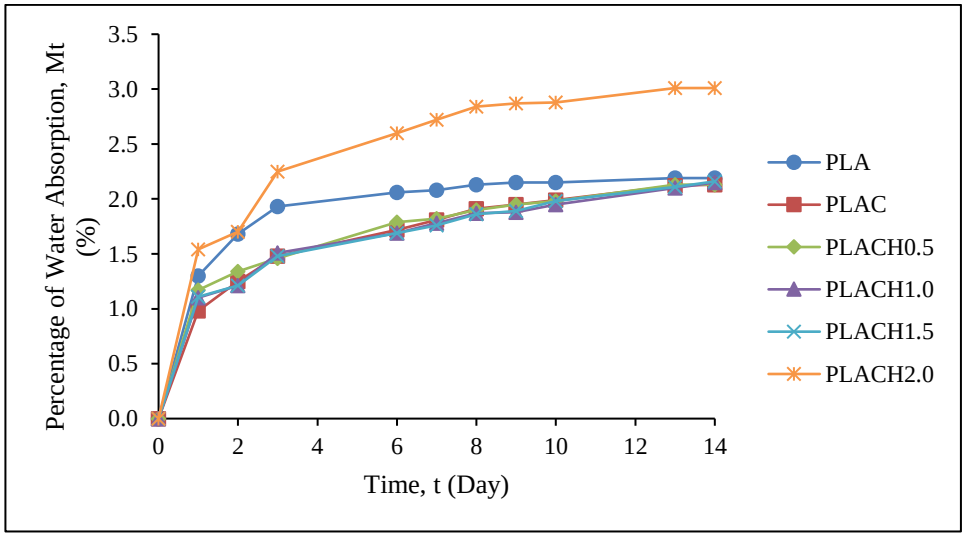

Figure 4 Water absorption of PLA and its nanocomposites at immersion temperature of 50 ℃

3.3 Biodegradability

Percentage of weight loss experienced by PLA and its nanocomposites were obtained after 122 days (17 weeks) of soil burial test, starting from 12th March 2020 to 12th July 2020, conducted at UTM Skudai, Johor. In this study, soil burial test was conducted to evaluate the biodegradability of PLA, PLA/CSR and PLA/CSR/HNT at different HNT content. In a soil burial test, the weight loss of a polymer is often taken to indicate the rate of degradation. The degradation of PLA is believed to follow a two-step mechanism. At first step, abiotic process takes place in which the water molecules diffuse into the materials and attack the ester linkages in PLA molecular structure, causing chemical hydrolysis of PLA and formation of water-soluble compounds, such as lactic acid. Hydrolysis of chains usually takes place at amorphous region due to the lower resistance to water attack. Next, biotic assimilation of polymer (by microorganisms) breaks down the products into water, carbon dioxide and biomass. The second step requires the presence of specific enzymes which are excreted by microorganisms such as bacteria, fungi and algae to activate the cleavage in the main chain of polyester and the residual fragments will be further utilized by the microorganisms as their source of energy [29,30].

Ideally, abiotic degradation takes place at the first step whereby the water molecules diffuse into the materials and attack the ester linkages in PLA molecular structure, causing the chemical hydrolysis of PLA. The highly hydrolysable ester bonds in PLA make this polymer highly subjected to degradation in humid environment, which favorable for biodegradation mechanism. Thus, the rate of biodegradation shows a close relationship with the water absorption ability of the PLA polyester as discussed earlier. In this study, it is well expected that the biodegradation rate of impact modified PLA to be increased with the increasing HNT content.

Table 3 shows the percentage of weight loss of PLA and its nanocomposites after soil burial test. In general, the soil burial test for all PLA nanocomposites showed a small weight loss (aproximately 1%) after 17 weeks of degradation time. From the result, it was found that the neat PLA recorded a percentage of weight loss of 0.15%. This finding was similar to a study reported by Lu et. al. [31], at which pure PLA only showed 0.1% of weight loss after 24 weeks of biodegradation test. According to Lu et. al. [31], the degradation rate of PLA in soil is slow compared to other biodegradable plastics because it is only susceptible to microbial attack by certain PLA-degrading microorganisms in natural environment such as *Amycolatopsis sp.* and *Saccharotrix sp.*, in spite of its biodegradability. It was clear that the degradation of PLA in soil is slow, subjecting to the availability of desired microorganisms and may take a long time for degradation to start in some conditions.

Referring to Table 3, a slight decrease of 0.04% in the percentage of weight loss was observed when CSR was incorporated into neat PLA. This phenomenon could be explained by the high molecular weight and crosslinks of CSR which physically retarded the degradation rate of PLA. However, the rate of degradation was slightly increased after HNT was incorporated into PLA/CSR in different content. Abdullah and Dong [32] also reported a slight increase of 4.52% in the biodegradation rate of polyvinyl alcohol/starch/glycerol/HNT nanocomposites at increasing HNT content from 1 wt% to 5 wt%, possibly due to the agglomeration of HNT. This may result in less restriction of mass transfer within the nanocomposite. It is well believed that prolonging the burial time could lead to higher degradation rate of nanocomposites.

Table 3 Percentage of weight loss of PLA and its nanocomposites after soil burial test

Material Designation	Percentage of weight loss (%)
PLA	0.15 ± 0.05
PLAC	0.11 ± 0.00
PLACH0.5	0.22 ± 0.01
PLACH1.0	0.26 ± 0.06
PLACH1.5	0.22 ± 0.01
PLACH2.0	0.26 ± 0.04

3.4 Thermogravimetry Analysis (TGA)

Single-stage decomposition was observed when PLA and its nanocomposites were analyzed under nitrogen atmosphere using TGA. The detail variation on the degradation temperature and the residual weight at 600 °C for PLA and its nanocomposites are summarized in Table 4.

Table 4 TGA results for PLA and its nanocomposites

Material Designation	Degradation Temperature (°C)			Residual weight at 600°C (%)
	$T_{5\%}$	$T_{10\%}$	T_{max}	
PLA	309.8	320	358.6	0
PLAC	281.7	292.4	332.5	0.696
PLACH0.5	308.2	320.4	356.5	1.313
PLACH2.0	308.9	320.6	354.1	2.135

Figure 5 shows (a) the effect of CSR on thermal stability of PLA and (b) the effect of HNT content on thermal stability of PLA/CSR. Based on TGA result, a neat PLA possess a $T_{5\%}$ and $T_{10\%}$ at 309.8 °C and 320 °C respectively, and a maximum decomposition rate at 358.6 °C. It was realized that the addition of CSR had caused the $T_{5\%}$, $T_{10\%}$ and T_{max} of neat PLA to be reduced to 281.7 °C, 292.4 °C and 332.5 °C respectively. However, it is noteworthy mentioning that the incorporation of HNT into PLA/CSR had led to an obvious increase in degradation temperature. In overall, incorporation of HNT at 2.0 phr showed the highest increment on $T_{5\%}$, $T_{10\%}$ and T_{max}, by 9.4%, 9.6% and 6.5% respectively. In addition, the residual weight percentage at 600°C also exhibited a significant increment of 1.44% when 2.0 phr of HNT was incorporated. The entrapment of degraded products into the lumen of HNT and the char residue formation could be a feasible explanation for the overall enhancement in the thermal stability of PLA/CSR in the presence of HNT [25]. It was suggested that those lumens in HNT could act as a barrier to hinder the diffusion of volatile losses. As a result, it could lead to a hindrance in mass transport, thereby increasing the thermal stability of PLA/CSR at higher content of HNT. This statement has received a common consent from other researchers [25,26].

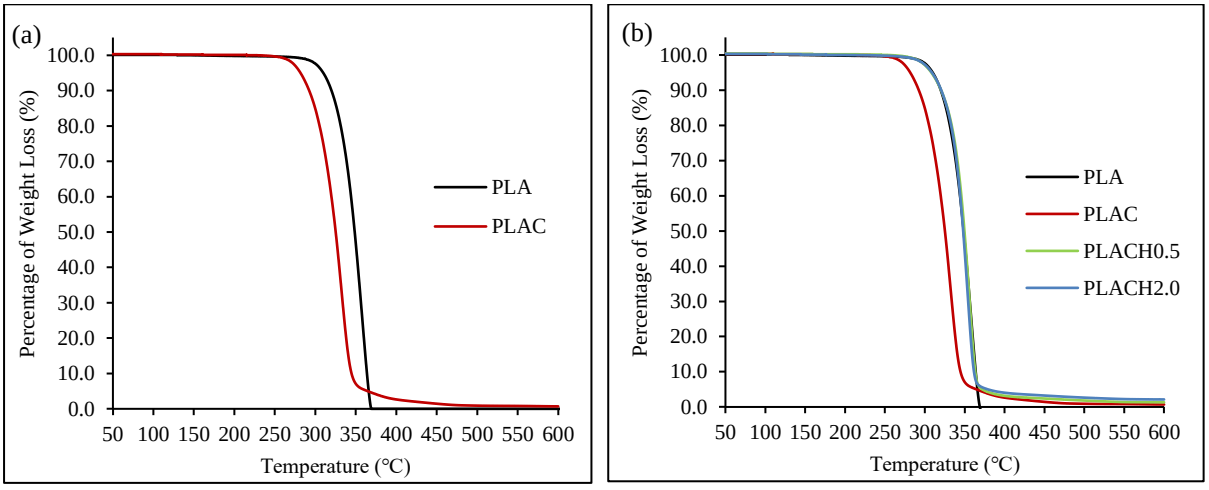

Figure 5 (a) Effect of CSR on thermal stability of PLA and (b) effect of HNT content on thermal stability of PLA/CSR

3.5 Differential Scanning Calorimetry (DSC)

DSC thermograms of PLA and its nanocomposites are shown in Figure 6 and their thermal characteristics are summarized in Table 5. Based on Table 5, neat PLA displayed a T_g at 58.0 °C, T_{cc} at 76.3 °C and T_m at 167.7 °C. The addition of CSR at 5 wt% only showed slight increment of 0.1 °C and 0.3 °C on the T_g and T_m of neat PLA respectively, almost not significant, which having similar observation as reported by Taib et. al. [23]. It was suggested that the PLA/impact modifier blends are immiscible, thus, thermal characteristics were commonly inherited from PLA matrix. On the other hand, the addition of CSR had significantly increased the T_{cc} of PLA from 76.3 °C to 101.7 °C. It is explained by the fact that the addition of impact modifier decreases the ability of PLA to crystallize and/or recrystallize [23]. Nevertheless, PLA/CSR was found to have lower degree of crystallinity than neat PLA. Therefore, it is obvious that the impact modifier might have inhibited the nucleation crystallization of PLA, as these molecules exist as melt state between the temperatures associated with cold crystallization of PLA [33].

Incorporation of HNT into PLA/CSR shows a moderate increase in T_g with increasing HNT content. Similar observation was reported by Wu et. al. [34]. This behavior could be attributed to the hindrance of migration and diffusion of PLA molecular chains by the increasing filler. Ideally, finely dispersed HNT could eventually magnify its nucleation effect and assist in the crystallization process of PLA [3]. This fact was proven when a shift in T_{cc} of PLA/CSR to a lower temperature was observed during the incorporation of 0.5 and 1.5 phr HNT. However, an unexpected behavior was noticed when T_{cc} of PLA/CSR/HNT at 1.0 and 2.0 phr HNT content were shifted to higher temperature and PLA/CSR/HNT at 1.0 phr HNT content showed two T_{cc} shoulder peaks at DSC scan. The possible reason could be attributed to the nanoclay loading and the extent of compatibility between and PLA matrix but a further investigation beyond the scope of this study is necessary to explain this unusual phenomenon.

In general, the incorporation of HNT led to a lower degree of crystallinity (χ_c) compared to PLA/CSR. The low χ_c could be due to HNT inhibit the crystallization of PLA in PLA/CSR and this effect is increased as HNT has good dispersion in the PLA/CSR matrix. According to Tham et. al [17], organoclay can inhibit the crystallization due to strong interaction between polymer matrix and organoclay, despite its nucleating effect, which might partially immobilize the polymer chain and hinder the crystallization process.

Table 5 Thermal characteristics of PLA and its nanocomposites recorded from DSC thermograms.

Material Designation	T_g (°C)	T_{cc} (°C)	T_m (°C)	χ_c (%)
PLA	58.0	76.3	167.7	42.7
PLAC	58.1	101.7	168.0	14.9
PLACH0.5	58.0	97.2	167.4	11.6
PLACH1.0	58.1	108.7	168.0	5.7
PLACH1.5	58.2	94.8	167.9	12.3
PLACH2.0	58.7	102.8	167.8	10.9

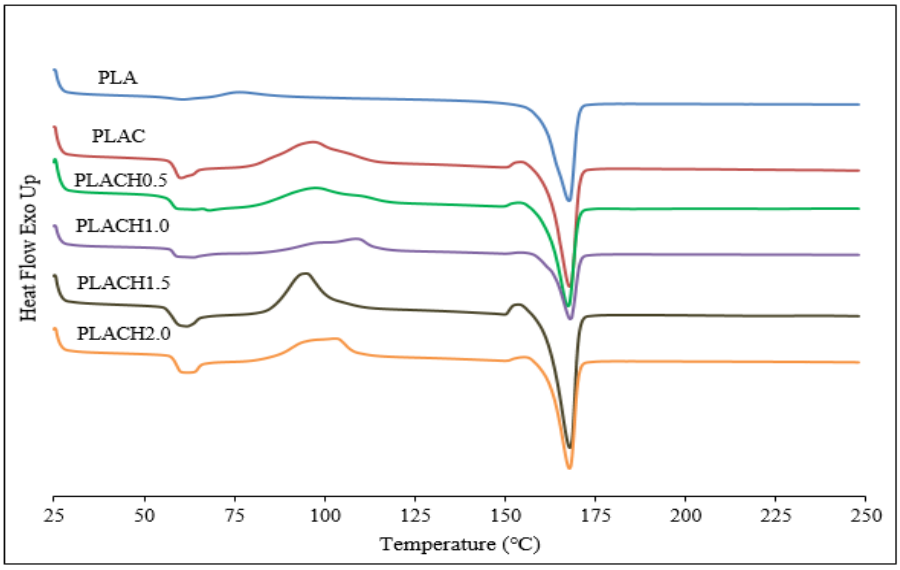

Figure 6 DSC thermograms of PLA and its nanocomposites

3.6 Fourier Transform Infrared Spectroscopy (FTIR) Analysis

Figure 7 shows the IR spectra of PLA and its nanocomposites. The emerging peak of PLA at 3508 cm^{-1} had attributed to the presence of terminal hydroxyl group (-OH) in PLA, while PLAC, PLACH0.5, PLACH1.0, PLACH1.5, and PLACH2.0 also recorded a corresponding stretching –OH peaks at 3513 cm^{-1}, 3648 cm^{-1}, 3647 cm^{-1}, 3647 cm^{-1}, and 3647 cm^{-1} respectively. The -OH peaks was not so significant after all, but it showed the same result with De Silva et. al. [25]. A higher wavenumber shifting (redshift) at O-H stretching in FTIR spectra of PLA/CH nanocomposites were observed. This redshift phenomenon occurred because siloxane group of HNT formed a hydrogen bonding with PLA's terminal hydroxyl groups, causing the –OH stretching peak to shift from 3508 cm^{-1} (neat PLA) to around 3647 cm^{-1} when HNT was incorporated. Moreover, the presence of C-H stretching vibration of CH_3 groups was confirmed

by the appearance of peaks at around 2996 cm^{-1} and 2946 cm^{-1} for each of the PLA nanocomposites. It is well known that the C=O and C-O peaks were the most obvious and disclosed immediate structural information if they were present in a FTIR spectra [35]. The identity of PLA polyester was further clarified when there was a strong C=O stretching absorption band at 1749 cm^{-1}, accompanied by a strong C-O stretching peak at 1181 cm^{-1}. These two evident peaks were also recorded by PLAC, and PLACH0.5 to PLACH2.0 as well. Nevertheless, a C-H bending peak was observed at 1453 cm^{-1}, followed by two O-H bending peaks at around 1382 cm^{-1} and 1360 cm^{-1} for all composite. It can be seen that PLACH0.5, PLACH1.0, PLACH1.5 and PLACH2.0 show a peak with increasing intensity (Inset 1) at 1043 cm^{-1}, 1044 cm^{-1}, 1043 cm^{-1} and 1044 cm^{-1} respectively. According to De Silva et. al [25], the increasing peak intensity at 1043 cm^{-1} was attributed to the overlapping of 1043 cm^{-1} with HNT's Si-O peak (in-plane stretching) at 1031 cm^{-1}. Therefore, this observation implies that Si-O groups of HNT could have form an interaction with PLA.

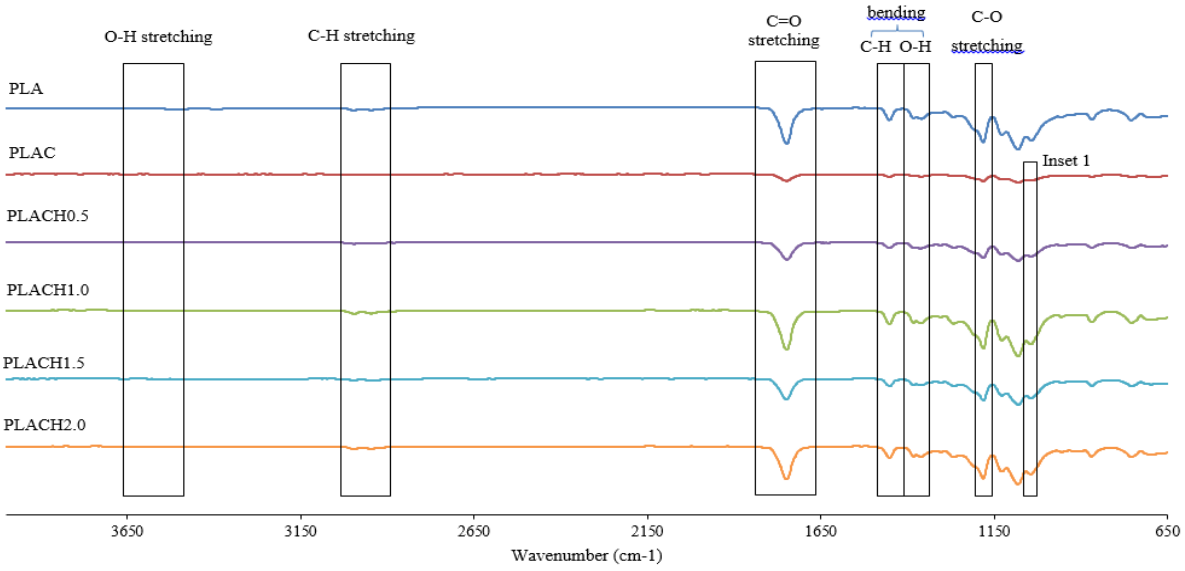

Figure 7 FTIR spectra of PLA and its nanocomposites; Inset 1: Increase of peak intensity due to overlapping with HNT's Si-O in-plane stretching peak

4.0 CONCLUSIONS

In this study, the effect of HNT on mechanical, physical and thermal properties of impact modified PLA was investigated. It is noteworthy mentioning that the incorporation of HNT at low content (i.e.: 0.5 phr and 1.0 phr) had successfully improved the mechanical properties of PLA/CSR. The improvement in flexural properties of impact modified PLA was attributed to the reinforcing effect of HNT. Inversely, a further addition in HNT content (1.5 phr and 2.0 phr) was found to reduce the flexural properties of PLA/CSR due to agglomeration, which causing

poor dispersion of HNT in PLA matrix and subsequently becoming stress concentration points. Moreover, incorporation of HNT had eventually increased the water absorption and biodegradability of PLA/CSR/HNT nanocomposites as the hydrophilic nature of HNT promoted interactions with water molecules. Ideally, higher water absorptivity favored the biodegradation of the polymer. The biodegradation of PLA/CSR/HNT nanocomposites were promoted with appreciable changes, probably because better interaction between water molecules and agglomerated HNT was established inside the polymer matrix to favored the hydrolytic cleavage. In addition, an improvement in thermal stability of PLA/CSR/HNT nanocomposites were observed. DSC results showed a decrease in the χ_c when HNT was incorporated into impact modified PLA. This could be possibly explained by the inhibition of crystallization by HNT and this effect was increased with good dispersion of HNT in PLA/CSR. FITR spectra showed some interaction between PLA/CSR matrix with HNT. In general, the incorporation of HNT at low content into impact modified PLA showed appreciable improvement on the mechanical, physical, and thermal properties of impact modified PLA. This study demonstrates that the optimum HNT content for maximum flexural strength and flexural modulus are at 1.0 phr and 0.5 phr respectively while 2.0 phr is required for maximum thermal stability.

Acknowledgement

The authors would like to express their appreciation to Faculty of Science and Faculty of Engineering, Universiti Teknologi Malaysia for providing the facilities and equipments.

REFERENCES

[1] Yu, L., Dean, K., and Li, L. (2006). Polymer blends and composites from renewable resources. *Progress in polymer science*, 31(6), 576-602.

[2] Lim, L.T., Auras, R., and Rubino, M. (2008). Processing technologies for poly (lactic acid). *Progress in polymer science*, 33(8), 820-852.

[3] Tham, W.L., Ishak, Z.M., and Chow, W.S. (2014). Mechanical and thermal properties enhancement of poly (lactic acid)/halloysite nanocomposites by maleic-anhydride functionalized rubber. *Journal of Macromolecular Science, Part B*, 53(3), 371-382.

[4] Wahit, M.U., Hassan, A., Ibrahim, A.N., Zawawi, N.A. and Kunasegeren, K. (2015). Mechanical, thermal and chemical resistance of epoxidized natural rubber toughened polylactic acid blends. *Sains Malaysiana*, 44(11), 1615-1623.

[5] Tanrattanakul, V., Jaratrotkamjorn, R., and Juliwanlee, W. (2020) Effect of maleic anhydride on mechanical properties and morphology of poly(lactic acid)/natural rubber blend. *Songklanakarin Journal of Science and Technology*, 42(3), 697-704.

[6] Amirabadi, S., Rodrigue, D., and Duchesne, C. (2018) Characterization of PLA-talc films using NIR chemical imaging and Multivariate Image Analysis techniques. *Polymer Testing*, 68, 61-69.

[7] Zotti, A., Zuppolini, S., Tabi, T., Grasso, M., Ren, G., Borriello, A., and Zarelli, M. (2018) Effects of 1D and 2D nanofillers in basalt/poly(lactic acid) composites for additive manufacturing. *Composites Part B: Engineering*, 153, 364-375.

[8] Petchwattana, N., Naknaen, P., and Narupai, B. (2020) Combination effects of reinforcing filler and impact modifier on the crystallization and toughening performances of poly(lactic acid). *eXPRESS Polymer Letters*, 14(9), 848–859.

[9] Mohd Din, S. F., Rashid, R. A., Saidi, M. A. A., and Othman, N. (2018) Mechanical, thermal and flammability properties of dolomite filled polypropylene composites. *PERINTIS eJournal*, 8(2), 58-73.

[10] Ezenkwa, O. E., Ismail, A. S., Saidi, M. A.A., Rashid, R. A., Hassan, A., and Arjmandi, R. (2019) mechanical and thermal properties of dolomite filled polycarbonate/acrylonitrile butadiene styrene composites. *PERINTIS eJournal*, 9(1), 1-14.

[11] Flynn, A., Torres, L. F., Hart-Cooper, W., McCaffrey, Z., Glenn, G. M., Wood, D. F., and Orts, W. J. (2020) Evaluation of biodegradation of polylactic acid mineral composites in composting conditions. *Journal of Applied Polymer Science*, 137(32), 48939.

[12] Du, M., Guo, B., and Jia, D. (2010). Newly emerging applications of halloysite nanotubes: a review. *Polymer International*, 59(5), 574-582.

[13] Du, M., Guo, B., Cai, X., Jia, Z., Liu, M., and Jia, D. (2008). Morphology and properties of halloysite nanotubes reinforced polypropylene nanocomposites. *e-Polymers*, 8(1).

[14] Du, M., Guo, B., Cai, X., Jia, Z., Liu, M., and Jia, D. (2008) Morphology and properties of halloysite nanotubes reinforced polypropylene nanocomposites. *e-Polymers*, 8(1), 130.

[15] Huang, Z. F., Jia, Z. X., Guo, B.C., and Jia, D. M. (2008) Structure and property of PBT/halloysite nano-tube composite. *China Plastics Industry*, 36, 29.

[16] Jia, Z., Luo, Y., Guo, B., Yang, B., Du, M., and Jia, D. (2009). Reinforcing and flame-retardant effects of halloysite nanotubes on LLDPE. *Polymer-Plastics Technology and Engineering*, 48(6), 607-613.

[17] Tham, W.L., Poh, B.T., Ishak, Z.M., and Chow, W.S. (2016). Epoxidized natural rubber toughened poly (lactic acid)/halloysite nanocomposites with high activation energy of water diffusion. *Journal of Applied Polymer Science*, 133(3).

[18] Lvov, Y. and Abdullayev, E. (2013). Functional polymer–clay nanotube composites with sustained release of chemical agents. *Progress in Polymer Science*, 38(10-11), 1690-1719.

[19] Thakore, I., Desai, S., Sarawade, B., and Devi, S. (2001). Studies on biodegradability, morphology and thermo-mechanical properties of LDPE/modified starch blends. *European Polymer Journal*, 37(1), 151-160.

[20] Leu, Y., Ishak, Z.M. and Chow, W.S. (2012). Mechanical, thermal, and morphological properties of injection molded poly (lactic acid)/SEBS-g-MAH/organo-montmorillonite nanocomposites. *Journal of applied polymer science*, 124(2), 1200-1207.

[21] Akbari, A., Jawaid, M., Hassan, A., and Balakrishnan, H. (2014). Epoxidized natural rubber toughened polylactic acid/talc composites: Mechanical, thermal, and morphological properties. *Journal of Composite Materials*, 48(7), 769-781.

[22] Aversa, C., Barletta, M., Gisario, A., Pizzi, E., Puopolo, M., and Vesco, S. (2018). Improvements in mechanical strength and thermal stability of injection and compression molded components based on Poly Lactic Acids. *Advances in Polymer Technology*, 37(6), 2158-2170.

[23] Taib, R.M., Ghaleb, Z., and Ishak, Z.M. (2012). Thermal, mechanical, and morphological properties of polylactic acid toughened with an impact modifier. *Journal of applied polymer science*, 123(5), 2715-2725.

[24] Liu, M., Jia, Z., Jia, D., and Zhou, C. (2014). Recent advance in research on halloysite nanotubes-polymer nanocomposite. *Progress in polymer science*, 39(8), 1498-1525.

[25] De Silva, R.T., Pasbakhsh, P., Goh, K.L., Chai, S.P., and Ismail, H. (2014). Synthesis and characterisation of poly (lactic acid)/halloysite bionanocomposite films. *Journal of Composite Materials*, 48(30), 3705-3717.

[26] Tham, W.L., Ishak, Z.M., and Chow, W.S. (2014). Water absorption and hygrothermal aging behaviors of SEBS-g-MAH toughened poly (lactic acid)/halloysite nanocomposites. *Polymer-Plastics Technology and Engineering*, 53(5), 472-480.

[27] Chow, W.S., Abu Bakar, A. and Ishak, Z.M. (2005). Water absorption and hygrothermal aging study on organomontmorillonite reinforced polyamide 6/polypropylene nanocomposites. *Journal of applied polymer science*, 98(2), 780-790.

[28] Ishak, Z.M. and Berry, J. (1994). Hygrothermal aging studies of short carbon fiber reinforced nylon 6.6. *Journal of applied polymer science*, 51(13), 2145-2155.

[29] Karamanlioglu, M. and Robson, G.D. (2013). The influence of biotic and abiotic factors on the rate of degradation of poly (lactic) acid (PLA) coupons buried in compost and soil. *Polymer degradation and stability*, 98(10), 2063-2071.

[30] Witt, U., Müller, R.J., and Deckwer, W.D. (1997). Biodegradation behavior and material properties of aliphatic/aromatic polyesters of commercial importance. *Journal of environmental polymer degradation*, 5(2), 81-89.

[31] Lu, H., Madbouly, S.A., Schrader, J.A., Srinivasan, G., McCabe, K.G., Grewell, D., and Graves, W.R. (2014). Biodegradation behavior of poly (lactic acid)(PLA)/distiller's dried grains with solubles (DDGS) composites. *ACS Sustainable Chemistry & Engineering*, 2(12), 2699-2706.

[32] Abdullah, Z.W. and Dong, Y. (2019). Biodegradable and water resistant poly (vinyl) alcohol (PVA)/starch (ST)/glycerol (GL)/halloysite nanotube (HNT) nanocomposite films for sustainable food packaging. *Frontiers in Materials*, 6, 58.

[33] Yeh, J.T., Tsou, C.H., Huang, C.Y., Chen, K.N., Wu, C.S., and Chai, W.L. (2010). Compatible and crystallization properties of poly (lactic acid)/poly (butylene adipate-co-terephthalate) blends. *Journal of Applied Polymer Science*, 116(2), 680-687.

[34] Wu, W., Cao, X., Zhang, Y., and He, G. (2013). Polylactide/halloysite nanotube nanocomposites: Thermal, mechanical properties, and foam processing. *Journal of Applied Polymer Science*, 130(1), 443-452.

[35] Coates, J. (2006). Interpretation of infrared spectra, a practical approach. *Encyclopedia of analytical chemistry: applications, theory and instrumentation*. USA: John Wiley & Sons, Ltd.